

RESEARCH PAPER

# Identification and characterization of a plastid-localized *Arabidopsis* glyoxylate reductase isoform: comparison with a cytosolic isoform and implications for cellular redox homeostasis and aldehyde detoxification

Jeffrey P. Simpson<sup>1,\*</sup>, Rosa Di Leo<sup>1,\*</sup>, Preetinder K. Dhanoa<sup>2</sup>, Wendy L. Allan<sup>1</sup>, Amina Makhmoudova<sup>1</sup>, Shawn M. Clark<sup>1</sup>, Gordon J. Hoover<sup>1</sup>, Robert T. Mullen<sup>2</sup> and Barry J. Shelp<sup>1,†</sup>

<sup>1</sup> Department of Plant Agriculture, University of Guelph, Guelph, Ontario, Canada N1G 2W1

<sup>2</sup> Department of Molecular and Cellular Biology, University of Guelph, Guelph, Ontario, Canada N1G 2W1

Received 9 November 2007; Revised 29 March 2008; Accepted 1 April 2008

## Abstract

Enzymes that reduce the aldehyde chemical grouping (i.e. H-C=O) to its corresponding alcohol could be crucial in maintaining plant health. Recently, recombinant expression of a cytosolic enzyme from *Arabidopsis thaliana* (L.) Heynh (designated as glyoxylate reductase 1 or AtGR1) revealed that it effectively catalyses the *in vitro* reduction of both glyoxylate and succinic semialdehyde (SSA). In this paper, web-based bioinformatics tools revealed a second putative GR cDNA (GenBank Accession No. AAP42747; designated herein as AtGR2) that is 57% identical on an amino acid basis to GR1. Sequence encoding a putative targeting signal (N-terminal 43 amino acids) was deleted from the full-length GR2 cDNA and the resulting truncated gene was co-expressed with the molecular chaperones GroES/EL in *Escherichia coli*, enabling production and purification of soluble recombinant protein. Kinetic analysis revealed that recombinant GR2 catalysed the conversion of glyoxylate to glycolate ( $K_m$  glyoxylate=34  $\mu$ M), and SSA to  $\gamma$ -hydroxybutyrate ( $K_m$  SSA=8.96 mM) via an essentially irreversible, NADPH-based mechanism. GR2 had a 350-fold higher preference for glyoxylate than SSA, based on the performance constants ( $k_{cat}/K_m$ ). Fluorescence microscopic analysis of tobacco (*Nicotiana*

*tabacum* L.) suspension cells transiently transformed with GR1 linked to the green fluorescent protein (GFP) revealed that GR1 was localized to the cytosol, whereas GR2-GFP was localized to plastids via targeting information contained within its N-terminal 45 amino acids. The identification and characterization of distinct plastidial and cytosolic glyoxylate reductase isoforms is discussed with respect to aldehyde detoxification and the plant stress response.

Key words: Aldehyde detoxification, cytosol, glyoxylate reductase, plastid, recombinant expression, redox homeostasis, subcellular localization, succinic semialdehyde reductase, transient expression.

## Introduction

Since plants are sessile organisms they require specialized metabolic pathways to respond to stress. Under some stresses, aldehydes accumulate in the plant and can be toxic due to their extreme reactivity (Kotchoni *et al.*, 2006). As a result, enzymes that reduce the aldehyde chemical grouping (i.e. H-C=O) to its corresponding alcohol are probably crucial in maintaining plant health. Recently, Shelp and co-workers (Breitkreuz *et al.*, 2003; Hoover *et al.*, 2007a, b) reported on the characterization of an *Arabidopsis* enzyme (designated hereinafter as glyoxylate

\* These authors contributed equally to the work.

† To whom correspondence should be addressed. E-mail: bshelp@uoguelph.ca

Abbreviations: BY-2, Bright Yellow-2; GABA,  $\gamma$ -aminobutyrate; GHB,  $\gamma$ -hydroxybutyrate; GR, glyoxylate reductase; GFP, green fluorescent protein; HEPES, 4-(2-hydroxyethyl)piperazine-1-ethanesulphonic acid; LB, Luria-Bertani; HIBADH, 3-hydroxyisobutyrate dehydrogenase; NAGK, N-acetyl glutamate kinase; ORF, open reading frame; PCR, polymerase chain reaction; RFP, red fluorescent protein; SDS-PAGE, sodium dodecyl sulphate-polyacrylamide gel electrophoresis; SSA, succinic semialdehyde.

reductase or GR1; EC 1.1.1.79) that catalyses the reduction of both glyoxylate and succinic semialdehyde (SSA), which are intermediates in the metabolism of glycolate and  $\gamma$ -aminobutyrate (GABA) metabolism, respectively. The corresponding *GR1* cDNA, which was identified by complementing a SSA dehydrogenase yeast mutant with an *Arabidopsis thaliana* cDNA library, enables this mutant to grow on GABA as the sole N source and significantly enhances the accumulation of  $\gamma$ -hydroxybutyrate (GHB), suggesting that the expressed protein converts SSA to GHB (Breitkreuz *et al.*, 2003). Kinetic studies of recombinant GR1 revealed that glyoxylate and SSA are reduced at physiological concentrations via an essentially irreversible NADPH-dependent reaction, although the enzyme prefers glyoxylate, and suggested that *in planta* activity is probably regulated by the ratio of NADPH/NADP<sup>+</sup> (Hoover *et al.*, 2007a, b).

In this paper, a search of the GenBank database with GR1 identified a second putative *Arabidopsis* GR cDNA, whose predicted amino acid sequence is 57% identical to GR1 (designated hereinafter as GR2). Sequence encoding a putative N-terminal targeting signal was removed from the full-length *GR2* cDNA and the truncated sequence was co-expressed with the molecular chaperones GroES/EL in *Escherichia coli*. Kinetic studies revealed that the substrate preference for purified recombinant GR2 was similar to that reported for GR1, although the actual affinity for both glyoxylate and SSA was an order of magnitude lower. Furthermore, both *GR1* and *GR2* were transiently expressed in tobacco Bright Yellow-2 (BY-2) suspension cells, revealing that GR1 localizes to the cytosol, whereas GR2 localizes to plastids. A companion paper reports on the stress-responsiveness of the GR isoforms, as well as GHB and related metabolites and redox levels, in *Arabidopsis* plants (Allan *et al.*, 2008).

## Materials and methods

### *Production, purification, and kinetic analysis of recombinant GR2*

The *A. thaliana* (L.) Heynh *GR1* cDNA (Accession No. AY044183) was blasted against the GenBank database and a full-length *Arabidopsis* cDNA sequence (Accession No. AAP42747), which is 57% homologous to GR1 at the amino acid level, was found. This sequence, designated as a putative GR2, was amplified from *Arabidopsis* ecotype Columbia mature rosette leaf cDNA with AmpiTaq DNA polymerase (Applied Biosystems, Foster City, CA, USA) according to the manufacturer's protocols. The full-length sequence was amplified using primers 5'-GGAATTCATATGATGGCTTTGTGCTCTATCTG-3' and 5'-CGCGGATCCAGCTTCTCGGGATTTTGC-3', which provided *NdeI* and *BamHI* restriction sites, respectively. A truncated cDNA sequence lacking the N-terminal 43 amino acids was amplified using primers 5'-GGAATTCATATGATGTCTACCAGAGATGAACTTGGAAC-3' and 5'-GGAATTCATATGAGCTTCTCGGGATTTTGC-3', which provided *NdeI* restriction sites on both ends. The amplified polymerase chain reaction (PCR) products (1039 and 910 bp, respectively) were cloned into the

pET-15b expression vector (Novagen, EMD Biosciences Inc., Madison, WI, USA) and sent to Genomics (University of Guelph, Laboratory Services Branch, Guelph, ON, Canada) for sequencing (ABI PRISM Sequencer Model 377, PerkinElmer Life Sciences, Foster City, CA, USA).

The GR2 constructs were expressed in *E. coli* BL-21(DE3) Rosetta (pLysS) cells (Novagen) co-expressing the GroES/GroEL chaperone complex (Dale *et al.*, 1994). To isolate recombinant GR2, the transformed cells were grown at 37 °C and 225 rpm in Luria-Bertani (LB) broth containing ampicillin (50 mg ml<sup>-1</sup>), chloramphenicol (34 mg ml<sup>-1</sup>), and kanamycin (30 mg ml<sup>-1</sup>) to an OD<sub>600</sub> of 0.6. The growing temperature of the culture was then reduced to 25 °C, and the cells were induced for 5 h by adding isopropyl- $\beta$ -D-thiogalactopyranoside to a final concentration of 0.25 mM. Then the cells were pelleted by centrifugation, weighed, and frozen at -20 °C.

Purified protein was obtained by suspending the frozen pellet in a TRIS-HCl (50 mM) buffer (pH 8.2) containing the protease inhibitors, phenylmethylsulphonyl-fluoride (1 mM), pepstatin A (1  $\mu$ g ml<sup>-1</sup>), and leupeptin (2  $\mu$ g ml<sup>-1</sup>). Soluble and insoluble cellular contents were separated by adding lysozyme (1 mg ml<sup>-1</sup>), MgCl<sub>2</sub> (50 mM), and a few DNase crystals and incubating the mixture on ice with gentle shaking for 1 h; 6 mM 3-[3-cholamido-propyl] dimethylammonio]-1-propanesulphonate was added after 30 min. Insoluble contents were pelleted by centrifugation and the resulting supernatant was passed over a nickel affinity column according to the manufacturer's protocols (Sigma-Aldrich, Oakville, ON, Canada). His<sub>6</sub>-tagged GR2 protein was eluted from the column in a TRIS-HCl (50 mM) buffer (pH 8.2) containing 500 mM imidazole and 10% glycerol, and immediately assayed for enzymatic activity as described below. Thereafter, the preparation was aliquoted and frozen at -80 °C, and thawed as necessary for detailed studies.

Denaturing 12% sodium dodecyl sulphate polyacrylamide gel electrophoresis (SDS-PAGE) (Laemmli, 1970) was used to visualize protein preparations. Immunoblotting was conducted according to standard protocols (Sambrook *et al.*, 1989) using the His-Tag monoclonal antibody (Novagen), the anti-mouse antibody (Sigma-Aldrich), and the alkaline phosphatase conjugate substrate kit (Bio-Rad Laboratories, Hercules, CA, USA) for detection. Molecular weight standards were purchased from Fermentas Life Sciences (Burlington, ON, Canada). Protein concentration was determined via the Bradford method (Bradford, 1976), using the assay kit provided by Bio-Rad Laboratories (Canada) Ltd.; bovine serum albumin (fraction V, Pierce) was used as the standard.

Enzymatic activity was measured by observing the oxidation or reduction of NADPH (designated as the forward and reverse reactions, respectively) at A<sub>340</sub> and 30 °C using a Beckman Du640 (Beckman Coulter Canada Inc., Mississauga, ON, Canada) or a Cary 300 (Varian Canada Inc., Mississauga, ON, Canada) double-beam absorption spectrophotometer. For the forward reaction, the 0.8 ml standard mixture contained 50 mM 4-(2-hydroxyethyl)piperazine-1-ethanesulphonic acid (HEPES) (pH 7.6), 20% sorbitol, 50  $\mu$ M NADPH, and 37.6 nM purified GR2. The reaction was initiated with 4.0 mM SSA or 50  $\mu$ M glyoxylate. Preliminary data were collected on the forward reactions using NADH and the reverse reactions (GHB  $\rightarrow$  SSA; glycolate  $\rightarrow$  glyoxylate) using NAD(P)<sup>+</sup>. For the forward reaction, NADPH was replaced with 50  $\mu$ M NADH. For the reverse reaction, HEPES and NADPH were replaced with 50 mM *N*-tris(hydroxymethyl)methyl-4-aminobutanesulphonic acid (pH 9.2) and 50  $\mu$ M NADP<sup>+</sup>, respectively, and the reaction was initiated with 7 mM GHB, 10 mM glycolate, or 10 mM 6-phosphogluconate.

Specific enzyme activity was a linear function of protein concentration from 2.2 nM to 35.4 nM. The optimal pH for enzyme activity was determined using buffers (50 mM) with overlapping

pH range (2-morpholino-ethanesulphonic acid for pH 5.5–6.8; HEPES for pH 6.8–8.2; *N*-tris(hydroxymethyl)methyl-4-aminobutanesulphonic acid for pH 8.2–9.6; and 3-(cyclohexylamino)-1-propanesulphonic acid for pH 9.7). The final pH was adjusted from 5.5–9.7 with HCl or NaOH.

Kinetic data were obtained for the forward (SSA → GHB and glyoxylate → glycolate) reactions by measuring initial rates (i.e. first 5 s) at fixed concentration of NADPH and varied concentrations of SSA or glyoxylate. All measurements were obtained in triplicate and the kinetic data were fit to the Michaelis–Menten equation ( $V = V_{\max}[S]/K_m + [S]$ ) using non-linear least square analysis (Sigma-Plot2000, version 6.1; Enzyme Kinetics Module, version 1.0). From the kinetic parameters ( $V_{\max}$ ,  $K_m$ ,  $k_{\text{cat}}$ ) a performance constant ( $k_{\text{cat}}/K_m$ ) was calculated for each substrate. A higher constant reveals the preferred substrate.

#### *Transient transformation of tobacco BY-2 cells and immunofluorescence microscopy*

Standard recombinant DNA procedures were performed as described by Sambrook *et al.* (1989). Molecular biology reagents were purchased from New England Biolabs (Mississauga, ON, Canada), Promega (Nepean, ON, Canada), Perkin-Elmer Life Sciences, Stratagene (La Jolla, CA, USA), or Invitrogen (Burlington, ON, Canada). Oligonucleotides were synthesized by Genologics. DNA was isolated and purified using reagent kits purchased from Qiagen (Mississauga, ON, Canada). All DNA constructs were sequenced using dye-terminated cycle sequencing by Genologics. Complete details of the oligonucleotide primers used in the gene cloning and plasmid constructions described below are available upon request.

Plant expression plasmids containing the *Arabidopsis GR1* and *GR2* open reading frames (ORFs) were constructed as follows. First, the *GR1* and *GR2* ORFs were amplified from pET15bGR1 and pET15bGR2, respectively, with appropriate forward and reverse primers that introduced *NcoI* or *NheI* restriction sites 5' and 3' of the *GR1* and *GR2* start and stop codons, respectively. The resulting PCR products were then gel-purified and subcloned into pCR2.1 (Invitrogen) to produce pCR2.1/*GR1* and pCR2.1/*GR2*. Next, pCR2.1/*GR1* and pCR2.1/*GR2* were digested with *NcoI* and *NheI*, respectively, and the resulting fragments were subsequently gel-purified and ligated into either *NcoI*-digested pUC18/*NcoI*-GFP (green fluorescent protein) or *NheI*-digested pUC18/*NheI*-GFP, pUC18/*GR1*-GFP and pUC18/*GR2*-GFP. pUC18/*NcoI*-GFP is a plant expression vector that includes the 35S cauliflower mosaic virus promoter and the GFP ORF immediately downstream from a unique in-frame *NcoI* site (Chiu *et al.*, 1996). pUC18/*NheI*-GFP is a modified version of pUC18/*NcoI*-GFP in which sequences corresponding to the *NcoI* site were altered (via PCR site-directed mutagenesis) to a *NheI* site.

pUC18/*GR2* 1-45-GFP was constructed by amplifying sequences in the *GR2* ORF that encoded for the protein's N-terminal 45 amino acid residues, including the predicted plastid targeting sequence (see Supplementary Fig. S1 at JXB online). pUC18/*GR2* Δ2-45-GFP was constructed by amplifying the *GR2* ORF, but without the protein's N-terminal 2-44 amino acid residues. Both amplicons were generated using PCR along with pET15bGR2 as template DNA and the appropriate forward and reverse mutagenic primers that introduced 5' and 3' *NheI* sites. For pUC18/*GR2* Δ2-45-GFP, the forward mutagenic primer also introduced sequences coding for an initiation (methionine) codon. The amplicon corresponding to *GR2* lacking its N-terminal 2-44 amino acid residues was subcloned into the pCR2.1 vector, followed by digestion with *NheI* and ligation into *NheI*-digested pUC18/*NheI*-GFP, yielding pUC18/*GR2* Δ2-45-GFP. Similarly, the PCR product consisting of the N-terminal 45 amino acids of *GR2* was digested with *NheI* and ligated directly into *NheI*-digested pUC18/*NheI*-GFP, yielding pUC18/*GR2* 1-45-GFP.

Construction of pRTL2/MCS-RFP-stop, encoding the full-length red fluorescent protein (RFP) and convenient 5' multiple cloning sites has been described elsewhere (Shockey *et al.*, 2006).

Tobacco (*Nicotiana tabacum* L. cv. BY-2) suspension-cultured cells were maintained and prepared for biolistic bombardment as described previously (Banjoko and Trelease, 1995). Briefly, transient transformations were performed using 5 μg of plasmid DNA with a biolistic particle delivery system 1000/HE (Bio-Rad Laboratories, Mississauga, ON, Canada). Bombarded cells were incubated for 20 h to allow for expression and sorting of the introduced gene, fixed in formaldehyde, incubated with 0.01% (w/v) pectolyase Y-23 (Kyowa Hakko Chemical Co., Chuo-ku Tokyo, Japan), and permeabilized with either 0.3% (v/v) Triton X-100 or 25 μg ml<sup>-1</sup> digitonin (Sigma-Aldrich Inc.) (Lee *et al.*, 1997).

Fixed and permeabilized cells were then incubated with the appropriate primary and secondary antibodies. Antibodies and sources were as follows: mouse anti-tubulin IgGs (Sigma-Aldrich Inc.); rabbit anti-N-acetyl glutamate kinase (NAGK) (kindly provided by Dr Greg Moorehead at the University of Calgary; Chen *et al.*, 2006); rabbit anti-GFP IgGs (Molecular Probes, Burlington, ON, Canada); goat anti-rabbit rhodamine red-X IgGs (Jackson ImmunoResearch Laboratories, West Grove, PA, USA); goat anti-rabbit Cy3 (Cedar Lane Laboratories, Burlington, ON, Canada); and goat anti-mouse Alexa 350 (Molecular Probes). Epifluorescent images of BY-2 cells were acquired using a Zeiss AxioScope 2 MOT epifluorescence microscope (Carl Zeiss Inc., Thornwood, NY, USA) with a Zeiss 63× Plan Apochromat oil-immersion objective. Image capture was performed using a Retiga 1300 charge-coupled device camera (Qimaging, Burnaby, BC, Canada) and Northern Eclipse 5.0 software (Empix Imaging Inc., Mississauga, ON, Canada). CLSM images of BY-2 cells were acquired using a Leica DM RBE (Leica Microsystems Inc., Richmond Hill, ON, Canada) microscope with a Leica 63× Plan Apochromat oil-immersion objective a Leica TCS SP2 scanning head, and the Leica TCS NT software package (version 2.61). Fluorophore emissions were collected sequentially in double-labelling experiments; single-labelling experiments exhibited no detectable crossover at the settings used for data collections. Confocal images were acquired as single optical sections and saved as 512×512 pixel digital images. All fluorescence images of cells shown in the figures are representative of >50 independent (transient) transformations from at least two independent transformation experiments. Figure compositions were generated using Adobe Photoshop CS (Adobe Systems Inc., Toronto, ON, Canada).

## Results

### *In silico identification of Arabidopsis GR2*

A search of the GenBank database with *GR1* enabled identification of a full-length *Arabidopsis* cDNA, which encodes a 343-amino acid polypeptide with a predicted molecular mass of 36.2 kDA, an isoelectric point of 8.54, a net charge of 4 at neutral pH, and 57% identity and 72% similarity to *GR1* (Fig. 1). Thus, the gene encoding the polypeptide has been designated as *AtGR2* for *A. thaliana* *GR2*. *GR2* possesses an additional 51 N-terminal amino acids compared to *GR1*, and analysis of this region using TargetP (Emanuelsson *et al.*, 2000), ChloroP (Emanuelsson *et al.*, 1999), and PSORT (Nakai and Kanehisa, 1992) (<http://www.expasy.org/tools/>) predicted the existence of a transit peptide that varied in length from 29 to 36 amino acids (Fig. 1), although the subcellular location of *GR2*

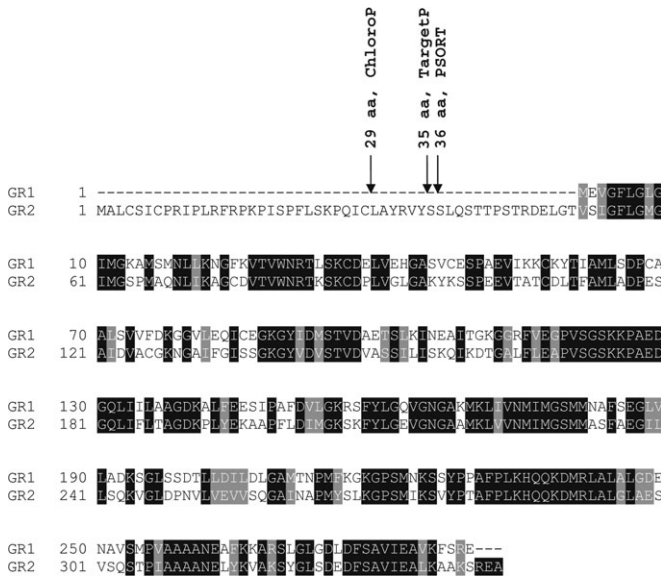


**Fig. 1.** ClustalW comparison of the predicted amino acid sequences for the full-length GR1 and GR2. Numbers indicate amino acid number. The first 51 amino acids in GR2 represent its putative targeting sequence, and the arrows indicate peptide cleavage sites as predicted by three web-based algorithms (ChloroP, TargetP, PSORT) for predicting subcellular localization. Identical and similar amino acids are shown by black and grey shading, respectively.

was ambiguous, with Predator (Small *et al.*, 2004) (<http://genoplante-info.infobiogen.fr/predotar/>), and TargetP favouring a mitochondrial location, and ChloroP and PSORT favouring a plastidial location (data not shown). As a compromise, in this study the N-terminal 43 (see ‘Production and characterization of recombinant *Arabidopsis* GR2’) or 45 (see ‘Transient expression and subcellular localization of *Arabidopsis* GR1 and GR2 in BY-2 cells’) amino acids were deleted from the full-length GR2 cDNA. The GR2 polypeptide has been tentatively identified as a 6-phosphogluconate dehydrogenase in The Arabidopsis Information Resource (<http://www.arabidopsis.org/>), but there is no published biochemical evidence to support such a function.

#### Production and characterization of recombinant *Arabidopsis* GR2

Both the full-length and truncated GR2 sequences were cloned into the pET15b vector, which was then introduced into *E. coli*. Only the recombinant truncated GR2 was soluble, and this was markedly improved by co-expression of the GroES/GroEL chaperone (Fig. 2A). Comparison of total protein from the lysates of cells transformed with the truncated gene insert (Fig. 2A) or with an empty insert (Fig. 2B) revealed a prominent band at approximately 35.9 kDa, the predicted size of the recombinant protein [31.4 kDa (300 amino acids) for the truncated sequence plus 2.18 kDa (20 amino acids) and 2.4 kDa

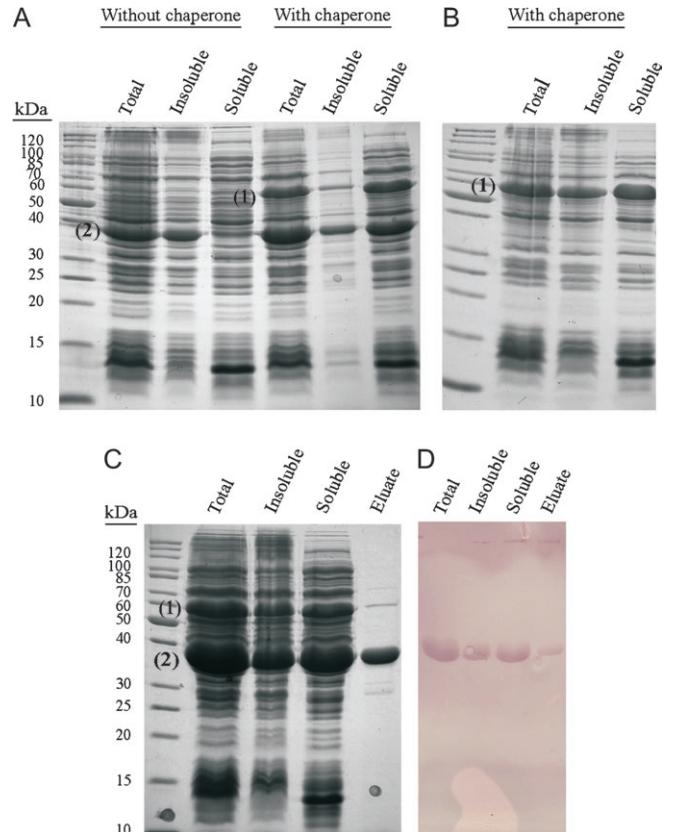


**Fig. 2.** Expression and purification of recombinant GR2 extracted from *E. coli* cells co-expressing the GroES/GroEL chaperone complex. The top row illustrates SDS-PAGE analysis of protein lysates from cells transformed with the truncated gene insert (A) or the empty insert (B), respectively, whereas the bottom row illustrates SDS (C) and immunoblot (D) analysis of protein lysates from cells transformed with the truncated gene insert. The gels were stained with Coomassie Blue, whereas the immunoblot was probed with an anti-His antibody. The EL subunit of the chaperone complex (1) and the recombinant protein (2) are indicated.

(23 amino acids) representing the N-terminal (including the His<sub>6</sub> epitope) and C-terminal flanking sequences translated from the pET-15B vector, respectively]. Therefore, soluble recombinant truncated GR2 for biochemical analysis was isolated from cells co-expressing the chaperone and subjected to affinity chromatography, enabling purification to near homogeneity (Fig. 2C). Immunoblot analysis of total protein, insoluble, soluble or purified protein, using an antibody against the His<sub>6</sub> tag, revealed a prominent band at approximately 35.9 kDa (Fig. 2D).

Enzyme activity was reasonably stable when the concentrated protein eluate from the affinity column was aliquoted and stored at  $-80^{\circ}\text{C}$  for months or at  $4^{\circ}\text{C}$  for hours. For enzyme assays, the protein eluate was diluted appropriately with elution buffer (see Materials and methods) so that the initial rate of reaction could be readily determined. During the assays, the diluted enzyme was stored at  $4^{\circ}\text{C}$ ; however, activity began to decrease

within 30 min. Therefore, multiple aliquots were required for detailed studies of pH and substrate specificity.

Maximal enzyme activity, which was determined with saturating glyoxylate and NADPH, was observed at pH 6.8 to 7.8 (Fig. 3); consequently, all subsequent assays were performed at pH 7.6. Preliminary assays of enzyme activity were conducted with, presumably, saturating concentrations of glyoxylate, SSA, glycolate, GHB, or 6-phosphogluconate and NADPH or NADP<sup>+</sup>. The protein catalysed the reduction of both glyoxylate and SSA using either NADPH or NADH as a cofactor; however, much greater activity was found with NADPH. For example, the reaction rate at 28  $\mu$ M glyoxylate and 50  $\mu$ M NADPH was 36 times faster than with glyoxylate and NADH at the same concentration. The enzyme also catalysed the reverse reaction involving GHB and NADP<sup>+</sup>, but at a lower rate than the forward reaction. For example, the rate with 7 mM GHB and 50  $\mu$ M NADP<sup>+</sup> was 170 times slower than the forward reaction with 7 mM SSA and 50  $\mu$ M NADPH. However, the enzyme was ineffective in

catalysing the reverse reaction utilizing either glycolate or 6-phosphogluconate. Thus, this polypeptide appears to be primarily dependent on NADPH and functions in an essentially irreversible manner.

Characterization of the forward reaction by varying the concentration of glyoxylate or SSA at saturating concentration of NADPH, and the concentration of NADPH at a saturating concentration of glyoxylate or SSA resulted in hyperbolic saturation kinetics, with Lineweaver–Burke and Eadie–Hofstee transformations of the data displaying linear dependence (plots not shown). Data from three independent enzyme preparations revealed that  $V_{\max}$  was similar for glyoxylate and SSA reduction, whereas the affinity for the two substrates was very different, with the  $K_m$  for glyoxylate being 130 times lower than that for SSA (Table 1). By contrast, the  $V_{\max}$  and  $K_m$  values for NADPH were similar in the presence of glyoxylate and SSA. Overall, the performance constants ( $k_{\text{cat}}/K_m$ ) revealed that the recombinant GR2 had a 350-fold higher preference for glyoxylate than SSA, but the preference for NADPH was unaffected by the preference for glyoxylate and SSA.

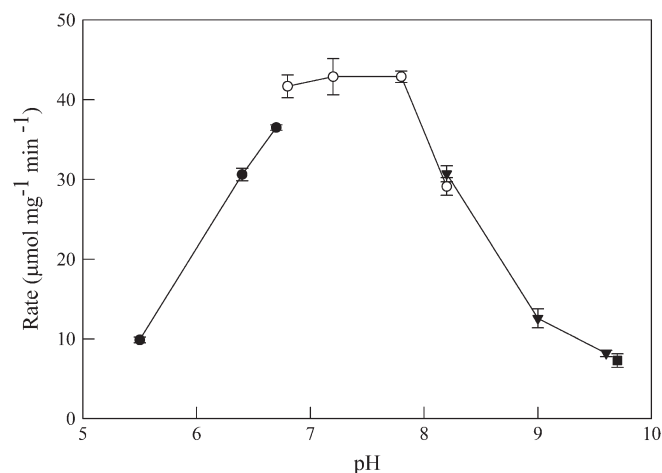


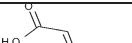
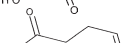
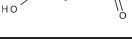

**Fig. 3.** Dependence of GR2 activity on pH. Activity was determined using saturating glyoxylate and NADPH as substrates, and 2-morpholino-ethanesulphonic acid (pH 5.5–6.8), HEPES (pH 6.8–8.2), *N*-tris(hydroxymethyl)methyl-4-aminobutanesulphonic acid (pH 8.2–9.6), and 3-(cyclohexylamino)-1-propanesulphonic acid (pH 9.7) as buffers. Data represent the mean  $\pm$ SE. of triplicate measurements from a typical enzyme preparation.

#### *Transient expression and subcellular localization of Arabidopsis GR1 and GR2 in tobacco BY-2 cells*

Tobacco BY-2 cells were co-transformed (via biolistic bombardment) with GR1-GFP, consisting of GR1 fused to the N-terminus of the GFP, and the RFP and examined using fluorescence microscopy. As shown in Fig. 4A, B the diffuse fluorescence pattern attributable to transiently-expressed GR1-GFP was similar to the fluorescence attributable to co-expressed RFP which lacks any inherent subcellular targeting information, indicating that GR1-GFP was localized throughout the cytosol. On the other hand, transient expression of GR2-GFP revealed that this fusion protein displayed a punctate and tubular-like fluorescence pattern that was similar to the fluorescence pattern attributable to endogenous NAGK (Fig. 4D), a well-characterized plastid stromal enzyme (Chen *et al.*, 2006). The co-localization between GR2-GFP and NAGK was also evident by the yellow colour in the merged image (Fig. 4E), indicating that GR2 is localized to plastids.

**Table 1.** Kinetic parameters for recombinant GR2

Kinetic data for varied substrate concentrations were best fit by non-linear regression analysis. Parameters represent the mean  $\pm$ SE of three independent enzyme preparations.

Varied substrate	Chemical structure of varied substrate	Fixed substrate	$K_m$ (mM)	$V_{\max}$ ( $\mu\text{mol min}^{-1} \text{mg}^{-1} \text{protein}$ )	$k_{\text{cat}}$ ( $\text{s}^{-1}$ )	$k_{\text{cat}}/K_m$ ( $\text{s}^{-1} \text{mM}^{-1}$ )
Glyoxylate		NADPH	$0.034 \pm 0.003$	$40.6 \pm 8.7$	$22.5 \pm 4.8$	$660 \pm 130$
NADPH		Glyoxylate	$0.0014 \pm 0.0002$	$23.0 \pm 2.2$	$12.0 \pm 0.8$	$8550 \pm 960$
SSA		NADPH	$8.96 \pm 0.71$	$30.7 \pm 4.0$	$17.0 \pm 2.2$	$1.89 \pm 0.27$
NADPH		SSA	$0.0012 \pm 0.0002$	$19.3 \pm 1.5$	$10.7 \pm 0.8$	$9180 \pm 1620$

As indicated above, web-based prediction analyses revealed the presence of a targeting signal peptide in the unique N-terminal extension of GR2, with the length of these predicted targeting peptides varying from 29 to 36 amino acids. As shown in Fig. 4 (F–H), the fusion protein GR2 1–45-GFP consisting of the N-terminal 45 amino acids of GR2 fused to GFP displayed a punctate and tubular-like fluorescence pattern that, similar to GR2-GFP (compare with Fig. 4C), co-localized with the fluorescence pattern attributable to endogenous plastidial NAGK. Deletion of the N-terminal 2–45 amino acids from GR2, however, resulted in the fusion protein (GR2  $\Delta$ 2–45-GFP) localizing throughout the cytosol (Fig. 4I) and not to plastids, as shown by the lack of co-localization of GR2  $\Delta$ 2–45 with endogenous NAGK (Fig. 4J). Overall, these data indicate that the N-terminal 45 amino acid residues of GR2 contain targeting information that is both sufficient and necessary for sorting the protein to plastids.

To determine whether GR2 was actually localized within plastids and not simply adjacent to the outside of the organelle, cells were differentially permeabilized with either triton X-100 or digitonin and then processed for immunofluorescence microscopy as above. triton X-100 permeabilizes all cellular membranes in BY-2 cells (Lee *et al.*, 1997), allowing the immunodetection with applied antibodies of protein epitopes located within the cytosol and within subcellular compartments. Digitonin, however, permeabilizes only the plasma membrane (Lee *et al.*, 1997), allowing for the immunodetection of cytosolic, but not intraorganellar epitopes. As illustrated in Fig. 5A and B, the fluorescence attributable to GR2-GFP was visible in both triton X-100- and digitonin-permeabilized cells due to the intrinsic fluorescence of the GFP moiety. However, when antibodies raised against the GFP moiety were used to detect GR2-GFP in the same transformed cells the immunofluorescence attributable to the expressed

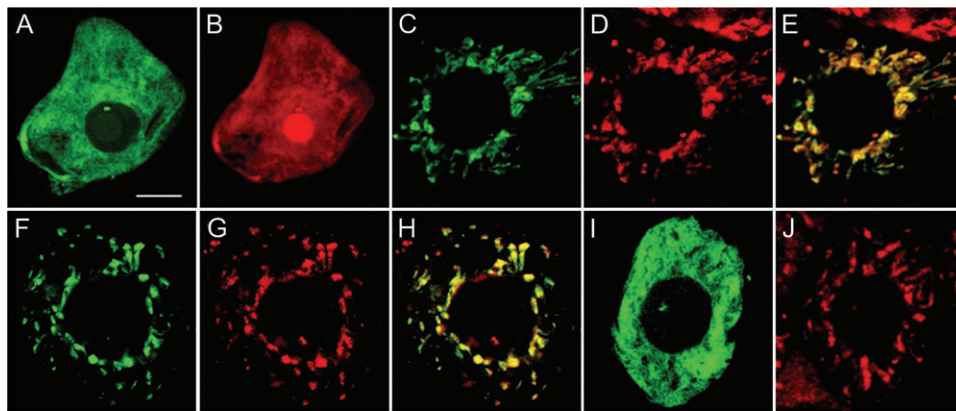


**Fig. 4.** Localization of GR1-GFP and GR2-GFP in transformed BY-2 cells. Images represent the localization of transiently-expressed or endogenous proteins in (co-) transformed (via biolistic bombardment) cells including (A) GR1-GFP and (B) RFP, (C) GR2-GFP and (D) NAGK, (F) GR2 1–45-GFP and (G) NAGK, and (I) GR2  $\Delta$ 2–45-GFP and (J) NAGK. (E) and (H) represent the corresponding merged images of the same cells shown in (C) and (D), and (F) and (G), respectively. Bar=10  $\mu$ m.

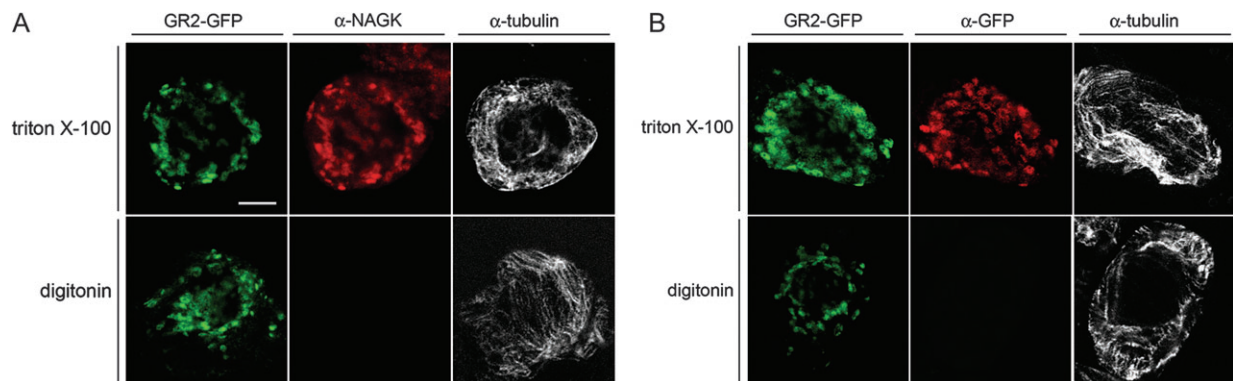


**Fig. 5.** Localization of GR2-GFP in differentially-permeabilized BY-2 cells. Images shown represent individual GR2-GFP-transformed cells that were fixed and permeabilized with either triton X-100 (top rows) or digitonin (bottom rows) and then immunostained with either (A) anti-NAGK and anti-tubulin or (B) anti-GFP and anti-tubulin antibodies. Note that in the GR2-GFP-transformed cells that were permeabilized with digitonin, neither endogenous NAGK, nor GR2-GFP, was immunostained. Bar=10  $\mu$ m.

fusion protein was observed in cells permeabilized with triton X-100, but not in cells permeabilized with digitonin (Fig. 5B). Similarly, control experiments revealed that, while endogenous NAGK was immunodetected in the same GR2-GFP transformed cells permeabilized with triton X-100, the endogenous stromal protein was not immunodetected in digitonin-permeabilized cells (Fig. 5A). Figures 5A and B also indicate that cytosolic tubulin was immunodetected in both triton X-100- and digitonin-permeabilized GR2-GFP-transformed cells as expected. Taken together, these data indicate that GR2, like NAGK, is localized within the plastid of BY-2 cells, presumably in the stroma.

## Discussion

### Identification of distinct cytosolic and plastidial GRs

Recently, a succinic semialdehyde dehydrogenase (SSADH)-deficient yeast mutant was complemented with an *A. thaliana* (L.) Heynh cDNA library, allowing the identification of a novel plant cDNA that encodes a 289-amino acid polypeptide with a subunit molecular mass of 30.3 kDa (designated herein as GR1) (Breitkreuz *et al.*, 2003). Constitutive expression of the cDNA in the mutant yeast enables growth on 20 mM GABA and significantly enhances the accumulation of GHB, suggesting that the expressed protein converts SSA to GHB (i.e. an aldehyde grouping to an alcohol). Kinetic analysis of substrate specificity revealed that the recombinant protein exhibits maximal activity near pH 7.8 and catalyses the conversion of glyoxylate to glycolate ( $K_m$  for glyoxylate=4.5  $\mu$ M,  $K_m$  for NADPH=2.2  $\mu$ M), as well as SSA to  $\gamma$ -hydroxybutyrate ( $K_m$  for SSA=0.87 mM,  $K_m$  for NADPH=2.6  $\mu$ M), via an essentially irreversible, NADPH-based mechanism (Hoover *et al.*, 2007a). Furthermore, the enzyme has a 250-fold higher preference for glyoxylate than SSA based on performance constants ( $k_{cat}/K_m$ ), and with the exception of 4-carboxybenzaldehyde, at least a 100-fold higher preference for SSA than all other substrates tested (formaldehyde, acetaldehyde, butyraldehyde, 2-carboxybenzaldehyde, glyoxal, methylglyoxal, phenylglyoxal, phenylglyoxylate). *In silico* analysis of subcellular localization suggested that GR1 is located in the cytosol. Together, these results suggest that, *in planta*, the protein would function in the conversion of SSA to GHB, as well as glyoxylate to glycolate.

In this report, a search of the GenBank database revealed a putative *Arabidopsis* GR2 cDNA, which encodes 343-amino acid polypeptide with a subunit molecular mass of 36.2 kDa (designated herein as GR2) (Fig. 1). Bioinformatic analysis of this polypeptide suggested that the 51-amino acid N-terminal extension of GR2 contained a targeting domain (Fig. 1), but it was unclear whether this signal conveyed mitochondrial and/or

plastidial localization. Transient expression in tobacco cells of GR1 and GR2, as well as modified versions of GR2, clearly showed that GR1 is localized to the cytosol, whereas GR2 is localized to plastids (Fig. 4). In addition, differential permeabilization results (Fig. 5) indicated that GR2 is not simply associated with the cytosolic face of the plastid's outer envelope membrane, but rather within the organelle, most likely the stroma.

Preliminary investigation revealed that soluble expression of a His-tagged, truncated recombinant GR2 that lacks the N-terminal 43 amino acids, was poor in *E. coli* cells that co-expressed the GroES/GroEL folding chaperone and were induced at 37 °C and 1 mM IPTG (data not shown). However, good soluble expression was obtained at 25 °C and 0.25 mM IPTG (Fig. 2). Presumably, this improvement in soluble recombinant protein expression could be attributed to a lower rate of synthesis and/or self-association (Zhang *et al.*, 1998). The recombinant protein, which was purified to near homogeneity using Ni<sup>2+</sup> affinity chromatography, exhibited maximal enzymatic activity for the conversion of glyoxylate to glycolate at slightly basic pH (Fig. 3). Since this pH optimum for the forward reaction is similar to that reported for GR1 (Hoover *et al.*, 2007a), it was assumed herein that the pH optima for the reverse reactions of GR2 and GR1 were also similar.

Activity measurements conducted at presumably saturating substrate levels revealed that recombinant GR2 could catalyse the interconversion of glyoxylate and glycolate and SSA and GHB via an NAD(P)H/NAD(P)<sup>+</sup>-based mechanism, but it is clear that the forward reactions were much more favourable than the reverse reactions and that NADPH was preferred over NADH as the co-factor, indicating that the reactions are biased towards the formation of glycolate or GHB in an essentially irreversible NADPH-dependent manner. Kinetic analysis revealed that the recombinant GR2 had a clear preference for glyoxylate ( $K_m$  for glyoxylate=34  $\mu$ M,  $k_{cat}/K_m$ =660 s<sup>-1</sup> mM<sup>-1</sup>) over SSA ( $K_m$  for SSA=9 mM,  $k_{cat}/K_m$ =1.9 s<sup>-1</sup> mM<sup>-1</sup>) (Table 1); however, the affinity of GR2 for both glyoxylate and SSA was an order of magnitude lower than that reported for GR1 (Hoover *et al.*, 2007a). Preliminary investigation revealed that some small and bulky molecules that are utilized poorly by GR1 (Hoover *et al.*, 2007a) were utilized even more weakly by GR2, if at all (JP Simpson, SM Clark, BJ Shelp, unpublished data). For example, in the presence of saturating NADPH, the  $K_m$  and  $k_{cat}/K_m$  values for glyoxal were 319 mM and 0.05 s<sup>-1</sup> mM<sup>-1</sup>, respectively.

Consequently, these studies represent the first descriptions of plant cDNAs that encode distinct cytosolic and plastidial isoforms of GR in *Arabidopsis*. Both GR1 and GR2 react with a chicken polyclonal antibody raised against a synthetic immunogenic peptide C GPVSGSK-KPA, which is based on amino acids 117–127 of the

*AtGR1* and 169–178 of the *AtGR2* (Hoover *et al.*, 2007a; JP Simpson, SM Clark, BJ Shelp, unpublished data). Earlier biochemical research revealed the existence of distinct cytosolic ( $K_m$  for glyoxylate of 70–100  $\mu\text{M}$ ) and chloroplastic ( $K_m$  for glyoxylate of 85  $\mu\text{M}$ ) NADPH-dependent GRs in spinach (Kleczkowski *et al.*, 1986; also see references in Givan and Kleczkowski, 1992). In spinach and pea, only about 10–20% of total leaf NADPH-dependent GR activity is located in chloroplasts (Givan and Kleczkowski, 1992).

#### Role of cytosolic and plastidial GRs during stress

The high affinity of recombinant GR2 ( $K_m=1.2\text{--}1.4\ \mu\text{M}$ ) (Table 1) and GR1 ( $K_m=2.2\text{--}2.6\ \mu\text{M}$ ) (Hoover *et al.*, 2007a) for NADPH and the high sensitivity of GR1 to competitive inhibition by the coenzyme product (Hoover *et al.*, 2007b) suggests that the ratio of NADPH/NADP<sup>+</sup> is probably a key factor regulating the activities of the two isoforms *in planta*. If so, both isoforms can theoretically contribute to redox homeostasis, as well as the detoxification of both glyoxylate and SSA, during stress (Allan *et al.*, 2003a, b; Breitkreuz *et al.*, 2003; Hoover *et al.*, 2007a) when elevated levels of cellular NADPH are present due to the activation of NAD(H) kinases (Harding *et al.*, 1997; Hunt *et al.*, 2004). The shift in redox components can limit the functioning of plastidial and mitochondrial electron transport chains (Scheibe *et al.*, 2005; Noctor, 2006), restrict the activity of enzymes such as SSA dehydrogenase (Fait *et al.*, 2005), and contribute to the accumulation of reactive oxygen species via NADPH oxidase (Hunt *et al.*, 2004).

Glyoxylate is a peroxisomal intermediate of glycolate metabolism, a pathway thought to serve a role in the dissipation of energy under conditions of high light and temperature (Wingler *et al.*, 2000). It can deactivate or slow the activation of ribulose biphosphate carboxylase/oxygenase, the primary enzyme involved in photosynthetic carbon reduction and photorespiratory carbon oxidation pathways (Campbell and Ogren, 1990). Givan and Kleczkowski (1992) proposed that a cytosolic GR is probably involved in scavenging glyoxylate so that any glyoxylate escaping transamination to glycine in the peroxisomes is neither lost irretrievably nor enters the chloroplasts and adversely affects photosynthesis, and the plastidial GR provides extra insurance. *In vitro* measurements revealed that recombinant GR1 (Hoover *et al.*, 2007a) and GR2 (Table 1) have affinities for glyoxylate that are in the physiological range (i.e. low micromolar range; Table 1), indicating that they probably function as GRs *in planta*.

By contrast, SSA is a mitochondrial intermediate of GABA metabolism, a pathway known to be stimulated under adverse environments (e.g. oxygen deficiency, cold and drought) and/or SSADH deficiency (Shelp *et al.*,

1999; Allan *et al.*, 2003a, b; Breitkreuz *et al.*, 2003; Bouché *et al.*, 2003; Fait *et al.*, 2005). Since the affinity of the two recombinant GRs for SSA is considerably lower than that for glyoxylate (i.e. the low millimolar range) (Hoover *et al.*, 2007a; Table 1), it is tempting to speculate that they are not involved in SSA metabolism *in planta*. However, recent research demonstrated that the accumulation of GHB, like GABA, is a general response to abiotic stress (i.e. salinity, drought, submergence, cold, heat), and that it is associated with the up-regulation of both *GR1* and *GR2* expression (Allan *et al.*, 2008). These findings are consistent with the hypothesis that *GR1* and *GR2* *in planta* are involved in the detoxification of SSA as well as glyoxylate. Currently, the metabolic functions of the GR isoforms are being investigated using various mutants of *Arabidopsis*.

#### Protein structure–function relationships for GR1 and GR2

A search of the GenBank database does not identify any non-plant GRs, nor any significant homology of the plant GRs with mammalian or bacterial NADPH-SSA reductases, although there is 22–31% identity to several known dehydrogenases, including tartronate semialdehyde reductase from *E. coli* (Accession no. P0ABQ2) (Hubbard *et al.*, 1998), 3-hydroxyisobutyrate dehydrogenase (HIB-ADH) from *Pseudomonas* (Accession no. P28811) (Steele *et al.*, 1992), and rat (Accession no. P29266) (Rougraff *et al.*, 1989), and 6-phosphogluconate dehydrogenase from *E. coli* (Accession no. P27754) (Jayaratne *et al.*, 1994), *Cunninghamella* (Accession no. O60037) (Wang *et al.*, 1998), sheep (Accession no. AAB20377) (O'N Somers *et al.*, 1992), maize (*Zea mays* L.) (Accession no. AAC27702) (Redinbaugh and Campbell, 1998) and spinach (*Spinacia oleracea* L.) (Accession no. AAK49817) (Krepinsky *et al.*, 2001). Based upon function, *AtGR1* and *AtGR2* could be designated as a NADPH-GR or NADPH-aldehyde reductase (EC 1.1.1.2), which includes SSA reductase (Hoover *et al.*, 2007a). Such enzymes typically belong to a large group of enzymes known as the aldo-keto reductases (the AKR superfamily; 28 November, 2006, <http://www.med.upenn.edu/akr>; Hyndman *et al.*, 2003), which are NAD(P) (H)-dependent and convert a variety of aldehydes and ketones to their corresponding alcohols. However, the similarity between the primary sequences of *GR1* and *GR2* and members of the AKR superfamily is low (Breitkreuz *et al.*, 2003; Hoover *et al.*, 2007a; this study), and the predicted secondary and tertiary structures of *GR1* and *GR2* do not meet AKR superfamily requirements (Hyndman *et al.*, 2003; GJ Hoover, BJ Shelp, unpublished results), suggesting that these proteins should not be included in the AKR superfamily. Moreover, the binding sites of *GR1* and *GR2* possess several amino acid residues



that are highly conserved and implicated in substrate binding in HIBADH and 6-phosphogluconate dehydrogenase (Breitkreuz *et al.*, 2003; Hoover *et al.*, 2007a; GJ Hoover, BJ Shelp, unpublished data), and the ordered Bi Bi kinetic mechanism for recombinant GR1 is consistent with that for members of both the AKR and HIBADH-related superfamilies of enzymes (Hoover *et al.*, 2007b), suggesting that GR1 and GR2 are members of the HIBADH-related superfamily of enzymes (Njau *et al.*, 2000, 2001). This hypothesis will be addressed elsewhere with detailed information about the crystal structure and putative catalytic site of GR1 (GJ Hoover, R Jorgensen, AR Merrill, BJ Shelp, unpublished data).

## Acknowledgements

This work was supported by funds to RTM and BJS from the Natural Sciences and Engineering Research Council of Canada, and to BJS from the Ontario Ministry of Agriculture and Food. RD, PKD, and SMC were recipients of an Ontario Graduate Scholarship.

## References

- Allan WL, Peiris C, Bown AW, Shelp BJ. 2003a. Gamma-hydroxybutyrate accumulates in green tea leaves and soybean sprouts in response to oxygen deficiency. *Canadian Journal of Plant Science* **83**, 951–953.
- Allan WL, Simpson JP, Clark SM, Shelp BJ. 2008.  $\gamma$ -Hydroxybutyrate accumulation in plants is a general response to abiotic stress: putative regulation by redox balance and glyoxylate reductase isoforms. *Journal of Experimental Botany* **59**, 2555–2564.
- Allan WL, Smith R, Shelp BJ. 2003b. Direct measurement of  $\gamma$ -hydroxybutyrate (GHB) in crude plant extracts by liquid chromatography/negative ion-ES mass spectrometry. Application Bulletin AB-0015. Mississauga, ON, Canada: Agilent Technologies Inc., 4 pp.
- Banjoko A, Trelease RN. 1995. Development and application of an *in vivo* plant peroxisome import system. *Plant Physiology* **107**, 1201–1208.
- Bouché N, Fait A, Moller SG, Fromm H. 2003. Mitochondrial succinic-semialdehyde dehydrogenase of the  $\gamma$ -aminobutyrate shunt is required to restrict levels of reactive oxygen intermediates in plants. *Proceedings of the National Academy of Sciences, USA* **100**, 6843–6848.
- Bradford MM. 1976. A rapid and sensitive method for the quantification of microgram quantities of protein utilizing the principle of protein–dye binding. *Analytical Biochemistry* **78**, 248–254.
- Breitkreuz KE, Allan WL, Van Cauwenberghe OR, Jakobs C, Talibi D, André B, Shelp BJ. 2003. A novel  $\gamma$ -hydroxybutyrate dehydrogenase. Identification and expression of an *Arabidopsis* cDNA and potential role under oxygen deficiency. *Journal of Biological Chemistry* **278**, 41552–41556.
- Campbell WJ, Ogren WL. 1990. Glyoxylate inhibition of ribulosebisphosphate carboxylase/oxygenase activation in intact, lysed, and reconstituted chloroplasts. *Photosynthesis Research* **23**, 257–268.
- Chen YM, Ferrar TS, Lohmeir-Vogel E, Morrice N, Mizuno Y, Beranger B, Ng KKS, Muench DG, Moorhead GBG. 2006. The PII signal transduction protein of *Arabidopsis thaliana* forms an arginine-regulated complex with plastid N-acetyl glutamate kinase. *Journal of Biological Chemistry* **281**, 5726–5733.
- Chiu W, Niwa Y, Zeng W, Hirano T, Kobayashi H, Sheen J. 1996. Engineered GFP as a vital reporter in plants. *Current Biology* **6**, 325–330.
- Dale GE, Schonfield HJ, Langen H, Stieger M. 1994. Increased solubility of trimethoprim-resistant type S1 DHFR from *Staphylococcus aureus* in *Escherichia coli* cells overproducing the chaperones GroEL and GroES. *Protein Engineering* **7**, 925–931.
- Emanuelsson O, Nielsen H, Brunak S, von Heijne G. 2000. Predicting subcellular localization of proteins based on their N-terminal amino acid sequence. *Journal of Molecular Biology* **300**, 1005–1016.
- Emanuelsson O, Nielsen H, von Heijne G. 1999. ChloroP, a neural network-based method for predicting chloroplast transit peptides and their cleavage sites. *Protein Science* **8**, 978–984.
- Fait A, Yellin A, Fromm H. 2005. GABA shunt deficiencies and accumulation of reactive oxygen intermediates: insight from *Arabidopsis* mutants. *FEBS Letters* **579**, 415–420.
- Givan CV, Kleczkowski LA. 1992. The enzymic reduction of glyoxylate and hydroxypyruvate in leaves of higher plants. *Plant Physiology* **100**, 552–556.
- Harding SA, Oh SH, Roberts DM. 1997. Transgenic tobacco expressing a foreign calmodulin gene shows an enhanced production of active oxygen species. *EMBO Journal* **16**, 1137–1144.
- Hoover GJ, Prentice GA, Merrill AR, Shelp BJ. 2007b. Kinetic mechanism of an *Arabidopsis* glyoxylate reductase: studies of initial velocity, dead-end inhibition and product inhibition. *Canadian Journal of Botany* **95**, 896–902.
- Hoover GJ, Van Cauwenberghe OR, Breitkreuz KE, Clark SM, Merrill AR, Shelp BJ. 2007a. Characteristics of an *Arabidopsis* glyoxylate reductase: general biochemical properties and substrate specificity for the recombinant protein, and developmental expression and implications for glyoxylate and succinic semialdehyde metabolism in planta. *Canadian Journal of Botany* **85**, 883–895.
- Hubbard BK, Koch M, Palmer DRJ, Babbit PC, Gerlt JA. 1998. Evolution of enzymatic activities in the enolase superfamily: characterization of the (D)-glucarate/galactarate catabolic pathway in *Escherichia coli*. *Biochemistry* **37**, 14369–14375.
- Hunt L, Lerner F, Zeigler M. 2004. NAD: new roles in signaling and gene regulation in plants. *New Phytologist* **163**, 31–44.
- Hyndman D, Bauman DR, Heredia VV, Penning TM. 2003. The aldo-keto reductase superfamily homepage. *Chemico-biological Interactions* **143**, 621–631.
- Jayaratna P, Bronner D, MacLachlan PR, Dodgson C, Kido N, Whitfield C. 1994. Cloning and analysis of duplicated *rfbM* and *rfbK* genes involved in the formation of GDP-mannose in *Escherichia coli* O9:K30 and participation of *rfb* genes in the synthesis of the group I K30 capsular polysaccharide. *Journal of Bacteriology* **176**, 3126–3139.
- Kleckowski LA, Randall DD, Blevins DG. 1986. Purification and characterization of a novel glyoxylate-reductase from spinach leaves. Comparison of immunological properties of leaf glyoxylate reductase and hydroxypyruvate reductase. *Biochemical Journal* **239**, 653–659.
- Kotchoni SO, Kuhns C, Ditzer A, Kirch HH, Bartels D. 2006. Over-expression of different aldehyde dehydrogenase genes in *Arabidopsis thaliana* confers tolerance to abiotic stress and protects plants against lipid peroxidation and oxidative stress. *Plant, Cell and Environment* **29**, 1033–1048.
- Krepinsky K, Plaumann M, Martin W, Schnarrenberger C. 2001. Purification and cloning of 6-phosphogluconate dehydrogenase from spinach. *European Journal of Biochemistry* **268**, 2678–2686.

- Laemmli UK.** 1970. Cleavage of structural protein during the assembly of the head of bacteriophage T4. *Nature* **227**, 680–685.
- Lee MS, Mullen RT, Trelease RN.** 1997. Oilseed isocitrate lyases lacking their essential type 1 peroxisomal targeting signal are piggybacked to glyoxysomes. *The Plant Cell* **9**, 185–197.
- Nakai K, Kanehisa M.** 1992. A knowledge base for predicting protein localization sites in eukaryotic cells. *Genomics* **14**, 897–911.
- Njau RK, Herndon CA, Hawes JW.** 2000. Novel  $\beta$ -hydroxyacid dehydrogenases in *Escherichia coli* and *Haemophilus influenzae*. *Journal of Biological Chemistry* **275**, 38780–38786.
- Njau RK, Herndon CA, Hawes JW.** 2001. New developments in our understanding of the  $\beta$ -hydroxyacid dehydrogenases. *Chemico-biological Interactions* **130–132**, 785–791.
- Noctor G.** 2006. Metabolic signaling in defense and stress: the central roles of soluble redox couples. *Plant, Cell and Environment* **29**, 409–425.
- O’N Somers D, Medd SM, Walker JE, Adam MJ.** 1992. Sheep 6-phosphogluconate dehydrogenase. *Biochemical Journal* **288**, 1061–1067.
- Redinbaugh MG, Campbell WH.** 1998. Nitrate regulation of the oxidative pentose phosphate pathway in maize (*Zea mays* L.) root plastids: induction of 6-phosphogluconate dehydrogenase activity, protein and transcript levels. *Plant Science* **134**, 129–140.
- Rougraff PM, Zhang B, Kuntz MJ, Harris RA, Crabb DW.** 1989. Cloning and sequence analysis of a cDNA for 3-hydroxyisobutyrate dehydrogenase. *Journal of Biological Chemistry* **264**, 5899–5903.
- Sambrook J, Fritsch EF, Maniatis T.** 1989. *Molecular cloning: a laboratory manual*, 2nd edn. Cold Spring Harbor, New York: Cold Spring Harbor Laboratory Press.
- Scheibe R, Backhausen JE, Emmerlich V, Holtgreffe S.** 2005. Strategies to maintain redox homeostasis during photosynthesis under changing conditions. *Journal of Experimental Botany* **56**, 1481–1489.
- Shelp BJ, Bown AW, McLean MD.** 1999. Metabolism and functions of gamma-aminobutyric acid. *Trends in Plant Science* **4**, 446–452.
- Shockey JM, Gidda SK, Chapital DC, Kuan JC, Dhanoa PK, Bland JM, Rothstein SJ, Mullen RT, Dyer JM.** 2006. Tung tree DGAT1 and DGAT2 have nonredundant functions in triacylglycerol biosynthesis and are localized to different subdomains of the endoplasmic reticulum. *The Plant Cell* **18**, 2294–2313.
- Small I, Peeters N, Legeai F, Lurin C.** 2004. Predotar: a tool for rapidly screening proteomes for N-terminal targeting sequences. *Proteomics* **4**, 1581–1590.
- Steele MI, Lorenz D, Hatter K, Perk A, Sokatch JR.** 1992. Characterization of the *mmsAB* operon of *Pseudomonas aeruginosa* PAO encoding methylmalonate-semialdehyde dehydrogenase and 3-hydroxyisobutyrate dehydrogenase. *Journal of Biological Chemistry* **267**, 13585–13592.
- Wang RF, Khan AA, Cao W-W, Cerniglia CE.** 1998. Identification and sequencing of a cDNA encoding 6-phosphogluconate dehydrogenase from a fungus, *Cunninghamella elegans* and expression of the gene in *Escherichia coli*. *FEMS Microbiology Letters* **169**, 397–402.
- Wingler A, Lea PJ, Quick WP, Leegood RC.** 2000. Photorespiration: metabolic pathways and their role in stress protection. *Philosophical Transactions of the Royal Society of London B* **355**, 1517–1529.
- Zhang Y, Olsen DR, Nguyen KB, Olson PS, Rhodes ET, Mascarenhas D.** 1998. Expression of eukaryotic proteins in soluble form in *Escherichia coli*. *Protein Expression and Purification* **12**, 159–165.